HHS Public Access

Author manuscript

Med Eng Phys. Author manuscript; available in PMC 2017 July 01.

Published in final edited form as:

Med Eng Phys. 2016 July ; 38(7): 656–663. doi:10.1016/j.medengphy.2016.04.009.

Pump function curve shape for a model lymphatic vessel

C.D. Bertram[1,*], **C. Macaskill**[1], and **J.E. Moore Jr.**[2]

[1]School of Mathematics and Statistics, University of Sydney, New South Wales, Australia 2006

[2]Department of Bioengineering, Imperial College, London, England SW7 2AZ

Abstract

The transport capacity of a contractile segment of lymphatic vessel is defined by its pump function curve relating mean flow-rate and adverse pressure difference. Numerous system characteristics affect curve shape and the magnitude of the generated flow-rates and pressures. Some cannot be varied experimentally, but their separate and interacting effects can be systematically revealed numerically. This paper explores variations in the rate of change of active tension and the form of the relation between active tension and muscle length, factors not known from experiment to functional precision. Whether the pump function curve bends toward or away from the origin depends partly on the curvature of the passive pressure-diameter relation near zero transmural pressure, but rather more on the form of the relation between active tension and muscle length. A pump function curve bending away from the origin defines a well-performing pump by maximum steady output power. This behaviour is favoured by a length/active-tension relationship which sustains tension at smaller lengths. Such a relationship also favours high peak mechanical efficiency, defined as output power divided by the input power obtained from the lymphangion diameter changes and active-tension time-course. The results highlight the need to pin down experimentally the form of the active tension/length relationship.

Keywords

numerical model; fluid-structure interaction; lymphangion; muscle mechanics; length-tension relation

1 Introduction

The lymphatic system scavenges water and protein from the body‘s interstitial spaces, returning them to the circulation at the subclavian veins. In the process it also collects foreign matter (particles, bacteria, viruses) which is brought into intimate contact with

[*]Corresponding author (phone +61-2-9351-3646, fax +61-2-9351-4534, ; Email: c.bertram@sydney.edu.au)

Declaration

The authors have no competing interests.

immune cells in lymph nodes. The lymphatic vessels of the gut have a specialised role in nutrient uptake.

The lymphatic vascular system consists of nonmuscular initial lymphatics where lymph is admitted via endothelial primary valves, and muscular collecting lymphatics. Collecting vessels consist of a series of lymphangions, contractile segments of vessel bounded by one-way valves. Thus each lymphangion is a pump. Analysis of intrinsic[1] lymphatic pumping begins by examining individual lymphangions, proceeding from there to networked structures. The clinical importance of achieving better understanding of lymphatic pumping rests primarily with the role of impaired pumping in lymphoedema. Impairment can arise from surgical interruption of the lymphatic conduit network or from radiation-induced lymphatic muscle dysfunction, but measurements of maximal pumping pressure show that there is also a wide range of pumping ability in normal volunteers [1].

The steady-state performance of any type of pump can be characterised by a single curve relating the mean flow-rate $\bar{Q}$ through the pump to the adverse pressure difference ΔP which the pump is overcoming. Generally, $\bar{Q}$ depends inversely on ΔP; thus, considering only positive flow-rates and outlet pressures higher than inlet, the pump function is expressed by a curve of negative slope intersecting the $\bar{Q}$ and ΔP axes. One intersection describes the adverse pressure difference which is just sufficient to stop the mean flow; the other describes the maximum possible flow-rate which would be achieved in the absence of all load on the pump, i.e. equal inlet and outlet pressures. Possible shapes corresponding to qualitatively different pumping abilities are shown in Figure 1.

Drake et al. [2] attributed a curve which bent inward toward the origin of $\bar{Q}$–ΔP coordinates to the onset at high vessel distension of active pumping, in a bed which had previously yielded lymph by extrinsic mechanisms alone (intermittent passive compression of lymphatic vessels from lung inflation and deflation). They attributed one which bent outward, away from the origin, to a Starling-resistor effect, i.e. the collapse of lymphatic vessels at low transmural pressure (Δp_{tm} = internal pressure p_m minus external pressure p_e). They also showed theoretically [3] that the parallel combination of two systems of lymph vessels would yield a curve bending inward toward the origin.

However there are many other possible influences. Given biological variability and the difficulty of the experiments, the subject of what and how many factors affect the shape of pump function curves is not readily explored empirically, but additional light can be shed through analysis of theoretical models [4–5]. The numerical model of two lymphangions in series by Venugopal et al. [4] displayed a perfectly linear relation between $\bar{Q}$ and ΔP. Bertram et al. [5] introduced an asymmetrically sigmoidal dependence of lymphangion diameter D on transmural pressure Δp_{tm}, which led to pump function curves which almost everywhere bent away from the origin, i.e. were concave as viewed from the origin. The $\bar{Q}$ −ΔP relation was shown to depend on the lymphangion transmural pressure, the offset from zero of the trans-valvular pressure difference at which valves changed state, the sharpness of the valve resistance-change function, and the two scale parameters of the passive pressure-

[1]There is also extrinsic pumping, whereby lymph transport occurs through the passive squeezing of lymphangions by adjacent tissue.

diameter relation. The $\bar{Q}$–ΔP relation rose to higher values of ΔP when the number of lymphangions (and valves) increased, and higher values of both ΔP and $\bar{Q}$ when the magnitude of the peak active tension increased.

Our model has since been developed to include (1) valves with switching hysteresis and Δp_{tm}-dependent bias to the open state [6], (2) a refractory period between contractions, (3) non-sinusoidal waveforms of activation, (4) the length-dependence[2] of active tension developed during contractions, and (5) parameter values tailored more closely to those measured in experiments on isolated lymphatic vessels of 100–250 μm diameter from rat mesentery. We therefore revisit the concept of the pump function curve and report on how some of these changes affect the curves, with particular reference to the question of whether the curves bend toward or away from the origin. As shown in Fig. 1, this has consequences for the maximum power which can be developed by a pump working within limits on maximum $\bar{Q}$ and ΔP which are likely to be set by fixed physiological properties. In pathological situations, these properties may change so as to diminish maximum $\bar{Q}$ and ΔP, or may combine with other facets of pumping so as to depress maximum power while preserving maximum $\bar{Q}$ and ΔP. Maximum power relates directly to the lymphatic intrinsic pumping reserve which is the mechanism of last resort to prevent interstitial swelling [7].

2 Methods

2.1 Description of the model

The equations of the single-lymphangion model are unchanged from Bertram et al. [8]; in brief,

$$\frac{dD}{dt}=\frac{2\left(Q_1-Q_2\right)}{\pi LD};\ p_1-p_{\mathrm{m}}=\frac{64}{\pi}\frac{\mu LQ_1}{D^4};\ p_{\mathrm{m}}-p_2=\frac{64}{\pi}\frac{\mu LQ_2}{D^4} \quad (1)$$

$$p_{i-1,2}-p_{i1}=R_{\mathrm{V}i}Q_i,\ \ i=1,2;\ R_{\mathrm{V}i}=R_{\mathrm{Vn}}+\frac{R_{\mathrm{Vx}}}{1+\exp\left(-s_{\mathrm{o}}\left(\Delta p_{\mathrm{V}i}-\Delta p_{\mathrm{o}i}\right)\right)};\ \Delta p_{\mathrm{V}i}=p_{i-1,2}-p_{i1} \quad (2)$$

$$p_{\mathrm{m}}-p_{\mathrm{e}}=f_{\mathrm{p}}\left(D\right)+f_{\mathrm{a}}\left(D,\mathrm{t}\right), \quad (3)$$

where i is valve number, $D(t)$ is diameter, t is time, $Q(t)$ is flow-rate (through a valve), L is lymphangion length, $p_1(t)$ / $p_{\mathrm{m}}(t)$ / $p_2(t)$ is the pressure at the upstream end/midpoint/

[2]Length here means circumference. With lymphangions assumed to remain circular, circumference is proportional to diameter. If collapse occurs, ‘diameter’ then has the sense of hydraulic diameter and retains the same relation to circumference. Thus a single relation between active tension and instantaneous diameter is added.

downstream end of the lymphangion, μ is lymph viscosity, $R_V(\Delta p_V)$ is the function describing valve resistance, Δp_V is the trans-valvular pressure drop, R_{Vn} is minimum valve resistance, $R_{Vn} + R_{Vx}$ is maximum valve resistance, $\Delta p_o(\Delta p_{tmv})$ is the pressure drop threshold for switching, Δp_{tmv} is valve transmural pressure[3], s_o is a constant determining the slope of $R_V(\Delta p_V)$ at $\Delta p_V = \Delta p_o$, p_e is external pressure, p_a (= p_{02}) is inlet reservoir pressure, p_b (= p_{21}) is outlet reservoir pressure, $f_p(D)$ is the curvilinear passive relation between $p_m - p_e$ and D, and $f_a(D, t)$ is the time-varying curve describing the contribution of active tension to the relation between $p_m - p_e$ and D. See Table 1 for the default values of constants in eqs. 1–3.

The passive and active $\Delta p_{tm}-D$ relationships, and the valve-switching arrangements, are described in sections 2.2 to 2.4.

2.2 Passive $\Delta p_{tm}-D$ relation

Our model has evolved through three forms of passive $\Delta p_{tm}-D$ relation, $f_p(D)$. The first was used by Bertram et al. [5] and in most results presented by Jamalian et al. [10]. A second, improved form (changing from negative to positive curvature at exactly $\Delta p_{tm} = 0$ and $D/D_d = 1$) was used for fig. 6 of Jamalian et al. [10][4]. A third form subsequently adopted [8] and used here was fitted to measured data of Δp_{tm} vs. D from Davis et al. [6]. All three are normalised by the pressure and diameter scaling parameters P_d and D_d respectively (P_d sets the local passive stiffness; D_d sets the size of the unpressurized and relaxed lymphangion). In practice the third form has always been used with quite different values of P_d and D_d from the other two, as part of a revision of parameter values to correspond with physiological data. It is shown in Fig. 2 (see section 2.4).

2.3 Valve properties

Bertram et al. [5] and Jamalian et al. [10] modelled normal lymphatic valve function with a fixed logistic curve[2] relating valve resistance nonlinearly to the trans-valvular pressure difference Δp_V. All results presented here use a more complex model [8–9], which incorporates the experimental findings of Davis et al. [6][5] as regards lymphatic valve hysteresis and transmural-pressure-dependent bias to the open state, to control the instantaneous value of the switching threshold Δp_o between open and closed states.

2.4 Length-tension relation

Maximum active muscular tension is a function of muscle length. This dependence was omitted in our original model [5]. There are relatively few data on the length-tension relation of lymphatic muscle [11–15]. Muscle length here relates to lymphatic diameter, and the available data for rat lymph vessels other than thoracic duct only span a range near the maximum diameter set by the passive elasticity. The mesenteric data [13] suggest that the contribution of active tension as a Δp_{tm}-term in the $\Delta p_{tm}-D$ relation is maximal near where

[3] Δp_{tm} has a specialised definition in the valvular context; see [9].
[4] Further results using the 2011 model, augmented with a refractory period between contractions and definition of a mid-lymphangion pressure, are archived on-line at http://arxiv.org/abs/1512.01269.
[5] Bertram et al. [8] showed that the closing data were almost certainly affected by an artefact relating to neglect of micropipette resistance, and applied a correction. This correction is also adopted here, giving rise to the parameter c_{fact}.

the passive vessel stiffness becomes very large; it must decline to zero at some lower diameter, but the data do not indicate how. We here investigate three continuously differentiable forms for the length/active-tension relation for contraction, as defined mathematically below. Form f_M0 was used previously [8]. Form f_M1 [16] employs extra constants to produce a quasi-linear increase of active tension with diameter, and form f_M2 maintains constant the active-tension contribution to pressure over most of the diameter range between $D = D_d$ (the diameter where $\Delta p_{tm} = 0$) and the maximum possible diameter enforced by passive stiffness. A piece-wise linear (i.e. not continuously differentiable) active-stress/strain relation somewhat resembling form f_M1 was employed by Reddy et al. [17].

The length-tension relation is a nonlinear function $M_d(D)$ relating circumferential active tension to diameter D, where, for f_M0 as used in Bertram et al. [8],

$$M_d(D) = M_0 \left(\frac{1}{1+\exp(-s_d(D - D_a))} + \frac{1}{1+\exp(s_d(D - D_b))} - 1 \right), \quad (4)$$

and $s_d = c_{Ms}/D_d$, $D_a = c_{Ma}c_9$, $D_b = c_{Mb}c_9$, and $c_9 = 0.02598$ cm is the passive-vessel diameter at 5 cmH_2O; $c_{Ms} = 3.25$, $c_{Ma} = 0.85$, and $c_{Mb} = 2$. This double logistic function describes active tension rising smoothly from zero at small D to a peak plateau value M_0, then falling smoothly back to zero at large D. Multiplied by a prescribed time-course $0 \le M_t(t) \le 1$ and divided by $D/2$, the time-varying active tension forms the component $f_a(D,t) = 2M_t(t)M_d(D)/D$ with dimensions of pressure of the constitutive relation (eq. 3) for the lymphangion[6].

The f_M1 relation modifies $M_d(D)$ such that the part describing active tension increasing with diameter is closer to linear, while remaining continuously differentiable. The modified curve was achieved by inserting a straight line having the gradient of the logistic function midpoint and passing through that point, then shrinking the two halves of the logistic function to fit in the remaining space between the ends of the line and the function asymptotes. Two new parameters are needed, namely the offsets from the midpoint of each half of the logistic function. The total curve thus employs six parameters: the position and slope of the rising ($D_a = c_{Ma}c_9$ and $s_{da} = c_{Msa}/D_d$) and falling ($D_b = c_{Mb}c_9$ and $s_{db} = c_{Msb}/D_d$) logistic functions (as before—see Bertram et al. [8] for definition of c_9 and D_d), plus the relative offsets y_{ua} and y_{da} for the rising logistic function. These parameters take the values $c_{Ma} = 0.77$, $c_{Msa} = 1.81$, $y_{da} = 0.8$, $y_{ua} = 0.5$, $c_{Mb} = 2$, $c_{Msb} = 3.25$.

The f_M2 relation multiplies the double logistic relation forming the outer parenthesis of eq. 4 by D, then renormalizes the result to a maximum of 1 before multiplication by M_0. Only the parameters of eq. 4 are needed, with new values $c_{Ma} = 0.325$; $c_{Mb} = 1.25$; $c_{Ms} = 7.5$. Figure 2 compares the f_M0, f_M1 and f_M2 forms of the length/active-tension relation.

[6]The f_M0 relation was defined by Bertram et al. [8], but its illustration in fig. 9(b) of that paper contained an error: for proper comparison with the passive pressure-diameter relation, the legend should have read "$2M_d(D)/D$, $M_0 = 250$ dyn cm^{-1}".

2.5 Rate of change of active tension

With the length-tension relation incorporated, active tension varies as $M(D,t) = M_d(D) \times M_t(t)$, where $M_t(t)$ is a waveform of tension development and decay vs. time t; a somewhat similar product formulation was used in the model of Reddy et al. [17]. In our original model [5], $M_t(t)$ was a continuous sinusoid, but contractions having the form $[1 - \cos(2\pi ft)]/2$ for $0 \le t \le 1/f$ are now separated by a refractory period t_r. We examine herein the effects of varying the rate of change of active tension within a contraction of given duration. The rate of change is governed by an extra parameter m. The effects of t_r and m on the $M_t(t)$ waveform are shown in Figure 3.

2.6 Other parameters

The parameter values are summarised in Table 1, which also indicates the typical ranges of ΔP and $\bar{Q}$ achieved in the resulting pump function curves. Each curve is the result of setting a number of values of $\Delta P = p_b - p_a$ (by varying p_b) and computing for each the cycle-average flow-rate $\bar{Q}$ which results. In general parameter values based more closely on observed rat mesenteric lymphatic vessels [8] lead to higher pressures but (as a result of the smaller diameter) lower flow-rates than in our original model [5]. We here focus on a model of one lymphangion; the behaviour of multi-lymphangion models is dominated by effects relating to the presence of multiple valves [16].

It is helpful to compute the work done on the fluid by the lymphangion, as

$$W_{in} = \pi L \oint M(D,t)\, dD. \quad (5)$$

The useful output work per cycle is $W_{out} = \Delta P\, \bar{Q}\, t_{cyc}$, where $t_{cyc} = 1/f + t_r$, and a mechanical efficiency of contraction can be defined as $\eta = W_{out}/W_{in}$.

3 Results

As described above, the evolution of the model has led to a situation where a single lymphangion can overcome much more adverse pressure than eight in series in our earlier model. On the other hand, the incorporation of measured degrees of valve bias to the open state leads under some circumstances to much regurgitation loss before valve closure. Such losses affect $\bar{Q}$ adversely, and thus overall pump function.

Increasing the diameter range over which significant contractile force could be sustained (forms f_M1 and f_M2) led to higher mean flow-rates over a wider range of ΔP (compare curves in Figure 4 sharing m-value). The rate-setting parameter m also increased pump performance importantly, in part due to the effects that sustained contraction had on valve operation. Consider initially the (blue) curve for f_M2 and $m = 1$, i.e. a continuously sinusoidal time-course of contraction onset and decay. At the extremes of a pump curve, pump function can be abnormal for reasons associated with the valves. When $\Delta P = 0$, there is no inlet/outlet adverse pressure difference to keep the valves closed, and they default to the open position except when a developing lymphangion contraction briefly causes

sufficient back-flow (and associated Δp_V) to close the inlet valve. There is regurgitation before closure, so the overall $\bar{Q}$ in this case is less than when there is moderate ΔP. At ΔP = 10 cmH_2O, contraction is ineffective. The pressure in the lymphangion rises above then sinks below p_b as D decreases then returns to its resting level, but never gets down to p_a, so the inlet valve stays shut, no fluid is taken in during diastole, and there is simply sloshing flow through the open outlet valve in systole.

The pump function curves of Fig. 4 indicate that increased contractility leads to increases in output work. In the process, more input work is done by contraction per cycle (Figure 5), and the mechanical efficiency of contraction accordingly varies differently from either (Figure 6). Again, consider initially the blue curve in each of these figures. Significant input work is done even when the mechanical efficiency of contraction is zero at $\Delta P = 0$, because there is intermittent flow through open valves offering a small but non-zero resistance. While $\bar{Q}$ is maintained at or near its peak value, input work rises approximately linearly with ΔP. The efficiency continues to climb even when input work begins to fall at ΔP = 8 cmH_2O. At ΔP = 10 cmH_2O, there is minuscule input work; since $\bar{Q}$ is finite and negative, the efficiency is numerically large and negative (not shown).

Consider now the full set of curves in Fig. 4. In the absence of a length/active-tension relation (see Supplement), the passive $\Delta p_{tm}-D$ relation was found to exert great influence on the shape of the pump function curve. When there is a length/active-tension relation, its form (Fig. 2) plays a vital role. The extent to which active tension maintains a maximal contribution to transmural pressure as contraction reduces the diameter determines both pump curve shape and the maximum values of ΔP that can be overcome and $\bar{Q}$ that can be attained (Fig. 4). Pump function can also be very significantly degraded by regurgitation prior to valve closure, because of the measured valve bias to the open state. This degradation can be limited by increasing the rate of contraction onset and decay, i.e. setting m = 2. With the f_M0 relation, forward flow is prevented altogether by regurgitation unless the rate of contraction onset is thus increased. With the f_M1 relation, the attainable values of both ΔP and $\bar{Q}$ are doubled by such a rate increase.

Relative to the $M_d(D)$ relation f_M2, the other two length/active-tension relations involve the muscle developing less active tension at most diameters. Consequently the input work is very much less with f_M0 or f_M1 (Fig. 5), but the mechanical efficiency of contraction is not greatly affected (Fig. 6). Conversely, the faster rate of onset and decay of active tension (m = 2) acts to cut down the extent of regurgitation, and therefore improves the efficiency of conversion of input work into output work in the form of time-averaged flow-rate in the face of adverse pressure. However this is evident only with f_M0 (where the ‘efficiency’ with m = 1 is negative) and f_M1. With f_M2, the efficiency when m = 2 exceeds that when m = 1 only at ΔP = 9 cmH_2O; at all other data-points where the efficiency is greater than zero, the $\bar{Q}$ gain is less than the increase in input work.

The reasons why η is higher when m = 1 with f_M2 for all $\Delta P < 9$ cmH_2O are quite complex, and illustrate well the interconnection of all the variables in the lymphangion model. The more leisurely onset of contraction allows regurgitation through the inlet valve (biased to remain open) to go on for longer before a sufficient rate of lymphangion volume reduction is

achieved to reach the valve closure threshold. With significantly more of the previous diastolic fill having been thus wasted, the subsequent isovolumic phase of contraction, before the outlet valve opens, occurs at a slightly lower diameter, and the next phase of contraction, when the outlet valve opens, also starts at a lower diameter. With everything happening on a slower time-scale, the instantaneous flow-rate out of the lymphangion at the time of reaching peak $M(D,t)$ is approximately half that when $m = 2$, and so the excess of pressure over p_b in the lymphangion at this time is correspondingly less. With less volume leaving the lymphangion per unit time, $D(t)$ is now descending slower than at $m = 2$, and at the time of peak $M(D,t)$ arrives at a value only very slightly less than at $m = 2$. However, the difference is sufficient, given the strong slope of the $M_d(D)$ relation, to cause the peak of $M(D,t)$ to be significantly lower.

The apex of the contraction having passed, its decay begins, and with the outlet valve still open, regurgitation occurs back into the lymphangion, increasing its diameter. Eventually the outlet valve closes, but, with a longer period of regurgitation having occurred at $m = 1$, the subsequent isovolumic relaxation period occurs at a significantly higher diameter than at $m = 2$. Recall that the input work is set by the area of the loop of $M(D,t)$ vs. D. The loop is now defined by lower $D(t)$ during isovolumic contraction, lower peak $M(D,t)$, and higher $D(t)$ during isovolumic relaxation; all three factors reduce the loop area, and the input work is 21% less than at $m = 2$. Owing to the increased regurgitation, $\bar{Q}$ is also less, but only 15% less, with peak $Q_1(t)$ and peak $Q_2(t)$ both somewhat more than half of what was achieved at $m = 2$. With ΔP the same, output work is proportional to $\bar{Q}$, so the efficiency is higher at $m = 1$.

4 Discussion

The unique and interesting biological pumping property of lymphatic vessel networks is not easily characterised experimentally, even at the level of a single lymphangion or vessel. Summarizing the main finding here, the shape of the pump function curve depends largely on the contribution of active tension to the constitutive relation between Δp_{tm} and D. In the absence of a length/active-tension relation, the constitutive relation linking time-varying transmural pressure and time-varying active tension is simply the passive $\Delta p_{tm}-D$ curve. When a length/active-tension relation is added to the model, its effects on the overall relation between Δp_{tm} and D predominate.

In particular, whether the pump function curve bends inward toward the origin or outward depends on the curvature of the $\Delta p_{tm}-D$ relation at $D = D_d$ and at low $\Delta p_{tm} > 0$. A pump for which the function curve bends away from the origin develops much more power at mid-level values of $\bar{Q}$ and ΔP than one for which it bends toward the origin (Fig. 1). Put another way, the pump for which the function curve bends toward the origin develops only a modest maximum power, given the values of $\bar{Q}$ and ΔP that it can attain at the extremes. Muscular lymphatic vessels are not necessarily set up to maximise power, but these considerations are appropriate to analysis of the lymphatic system‘s pumping capacity, which in turn bears on its ability to deliver physiological goals such as homeostasis in the face of unusually large fluid loading or (e.g.) pathologically increased capillary leakage. Similarly, the question of

mechanical efficiency of pumping bears on the metabolic energy usage of the system when transporting lymph by intrinsic pumping.

When an active-tension/length relation is included in the model, its effects dominate over those of the passive $\Delta p_{tm}-D$ relation. Relative to small arteries and veins, the active-tension contribution to pressure scarcely declines before the passive curve reaches the point where further diameter increase becomes virtually impossible [13]. How active tension declines to zero at small length has not been defined experimentally for rat mesenteric lymphatics. The form f_M2 (Fig. 2) provides a constant contribution to transmural pressure from active tension over much of the diameter range between $D = D_d$ and where high vessel stiffness prevents further D-increase. With the overwhelming effect of length-dependent active tension thus removed, the influence of the passive $\Delta p_{tm}-D$ relation is again seen. The form of the passive $\Delta p_{tm}-D$ relation fitted to measured data of a lymphatic vessel [8] also displays negative curvature at $D = D_d$ and at low $\Delta p_{tm} > 0$. Consequently, the combination of this form with f_M2 again gives rise to pump function curves bending prominently away from the origin (Fig. 4). The rapid increase in stiffness ($d\Delta p_{tm}/dD$) at the right-hand side of the passive $\Delta p_{tm}-D$ relation is shown by these results not to be necessary for obtaining $\bar{Q}-\Delta P$ curves which bend away from the origin.

Conversely, the pump curve no longer bends away from the origin when the length/active-tension relation is f_M0 or f_M1; cf. Figs. 2 and 4. Under these circumstances, most of the pump function curve is fairly linear; only at $\Delta P = 0$ where valves tend to remain open do the curves depart notably from linearity.

As noted previously [8], the measured bias of the valves to staying open gives great importance in the model to the value of the open-valve resistance, which sets how much back-flow is needed to overcome the bias and close the valve. It also means that the efficacy of pumping acquires a strong dependence on the rate of change of active tension, as controlled by the parameter m (Figs. 4–6), because higher rates cause this back-flow to be achieved sooner. Were it not for the valve bias, m would be expected to have minimal importance, given the negligible fluid inertia in these tiny vessels. The lack of inertia means that there is no significant advantage in maintaining a contraction; in other model runs not shown here, we find only insignificant differences in output per cycle between runs with $m = 2$ and $f = 0.5$ Hz and those with $m = 1$ and $f = 1$ Hz (i.e. the same rate of change of active tension but without the pause at maximal contraction). This finding of course presupposes a refractory period long enough that contractions are effectively isolated from each other; otherwise, considerations of incomplete diastolic filling may intervene.

Most experimental data from (e.g.) Davis et al. [6] concentrate on how the amplitude, etc., of contractions vary in response to (e.g.) slow variations in the controlled parameters such as inlet and outlet pressure. However, lymphangion diameter or pressure for a single contraction typically exhibits a short-lived systolic plateau, suggesting the possibility that peak activation is maintained for a short while before it decays. Based on these observations we have varied m between 1 and 2, spanning the likely range, and in the process usefully focusing on a variable that has not been accessed experimentally thus far.

There are significant limitations involved in any experimental or modelling evaluation of lymphatic pumping function. The small dimensions involved (diameters, pressures, flow-rates) present considerable experimental challenges. Consequently there are gaps in what is known, which can be filled in a model by means of analytical approximations. The lack of experimental characterisation of some parameters represents a continuing limitation on the applicability of our results. Furthermore, lymphatic contractions are myogenic in the sense that contraction is triggered by diastolic vessel distension [18], causing the frequency of contraction to depend on the distending pressure; this regulatory influence is absent from our model as reported herein.

The range of length/tension relations examined here numerically leads to wide variations in the predicted shape of the pump function curve (Fig. 4). Experimentally (see Figure 7), curves show a similarly wide range of shapes, from convex to concave toward the origin as in Fig. 1. Evidence from the experiments of Eisenhoffer et al. [20–21] offers support for simulated pump function curves that bend away from the origin (panels b and c). This may indicate that the f_M2 form for the length/active-tension relation indeed emulates the real extent to which active tension is maintained down to $D = D_d$. Of all the factors involved in lymphangion pumping, the behaviour of active tension is the least well understood and characterised. The technique usually used to investigate it so far, namely, subtracting a passive $\Delta p_{tm}-D$ relation from a contracted $\Delta p_{tm}-D$ relation at corresponding diameters [13–14], leaves much of the length/active-tension relation unexplored, since the contracted relation typically extends to much smaller diameters. Further experimental investigation is clearly needed, of this and of the extent to which the passive $\Delta p_{tm}-D$ relation and the active contribution can vary between individual vessels.

Acknowledgments

JEM gratefully acknowledges support from U.S. National Institutes of Health grant R01-HL-094269, the Royal Academy of Engineering and a Royal Society-Wolfson Research Merit Award. All authors acknowledge support from U.S. National Institutes of Health grant U01-HL-123420.

References

1. Sugisawa R, Unno N, Saito T, Yamamoto N, Inuzuka K, Tanaka H, et al. Effects of compression stockings on elevation of leg lymph pumping pressure and improvement of quality of life in healthy female volunteers: a randomized controlled trial. Lymphatic Research and Biology. 2016
2. Drake R, Giesler M, Laine G, Gabel J, Hansen T. Effect of outflow pressure on lung lymph flow in unanesthetized sheep. Journal of Applied Physiology. 1985; 58:70–6. [PubMed: 3968025]
3. Drake RE, Allen SJ, Katz J, Gabel JC, Laine GA. Equivalent circuit technique for lymph flow studies. American Journal of Physiology (Heart and Circulatory Physiology). 1986; 251:H1090–H4.
4. Venugopal AM, Stewart RH, Laine GA, Dongaonkar RM, Quick CM. Lymphangion coordination minimally affects mean flow in lymphatic vessels. American Journal of Physiology - Heart and Circulatory Physiology. 2007; 293:H1183–H9. [PubMed: 17468331]
5. Bertram CD, Macaskill C, Moore JE jr. Simulation of a chain of collapsible contracting lymphangions with progressive valve closure. ASME J Biomech Eng. 2011a; 133:011008. 1–10.
6. Davis MJ, Rahbar E, Gashev AA, Zawieja DC, Moore JE jr. Determinants of valve gating in collecting lymphatic vessels from rat mesentery. American Journal of Physiology - Heart and Circulatory Physiology. 2011; 301:H48–H60. [PubMed: 21460194]
7. Aukland K. Why don't our feet swell in the upright position? News in Physiological Sciences. 1994; 9:214–9.

8. Bertram CD, Macaskill C, Davis MJ, Moore JE jr. Development of a model of a multi-lymphangion lymphatic vessel incorporating realistic and measured parameter values. Biomechanics and Modeling in Mechanobiology. 2014; 13:401–16. [PubMed: 23801424]
9. Bertram CD, Macaskill C, Moore JE jr. Incorporating measured valve properties into a numerical model of a lymphatic vessel. Computer Methods in Biomechanics and Biomedical Engineering. 2014; 17:1519–34. [PubMed: 23387996]
10. Jamalian S, Bertram CD, Richardson WJ, Moore JE jr. Parameter sensitivity analysis of a lumped-parameter model of a chain of lymphangions in series. American Journal of Physiology - Heart and Circulatory Physiology. 2013; 305:H1709–H17. [PubMed: 24124185]
11. Ohhashi T, Azuma T, Sakaguchi M. Active and passive mechanical characteristics of bovine mesenteric lymphatics. American Journal of Physiology (Heart and Circulatory Physiology). 1980; 239:H88–H95.
12. Ferguson MK, Williams U, Leff AR, Mitchell RW. Length-tension characteristics of bovine tracheobronchial lymphatic smooth muscle. Lymphology. 1993; 26:19–24. [PubMed: 8464221]
13. Zhang R-Z, Gashev AA, Zawieja DC, Davis MJ. Length-tension relationships of small arteries, veins, and lymphatics from the rat mesenteric microcirculation. American Journal of Physiology - Heart and Circulatory Physiology. 2007; 292:H1943–H52. [PubMed: 17172274]
14. Gashev AA, Zhang R-Z, Muthuchamy M, Zawieja DC, Davis MJ. Regional heterogeneity of length-tension relationships in rat lymph vessels. Lymphatic Research and Biology. 2012; 10:14–9. [PubMed: 22416912]
15. Caulk AW, Nepiyushchikh ZV, Shaw R, Dixon JB, Gleason RL jr. Quantification of the passive and active biaxial mechanical behaviour and microstructural organization of rat thoracic ducts. Journal of the Royal Society - Interface. 2015; 12:20150280.
16. Bertram CD, Macaskill C, Davis MJ, Moore JE jr. Consequences of intravascular lymphatic valve properties: a study of contraction timing in a multi-lymphangion model. American Journal of Physiology - Heart and Circulatory Physiology. 2016; 310 in press.
17. Reddy NP, Krouskop TA, Newell PH jr. A computer model of the lymphatic system. Computers in Biology and Medicine. 1977; 7:181–97. [PubMed: 891141]
18. Gashev AA, Davis MJ, Delp MD, Zawieja DC. Regional variations of contractile activity in isolated rat lymphatics. Microcirculation. 2004; 11:477–92. [PubMed: 15371129]
19. Venugopal AM, Quick CM, Laine GA, Stewart RH. Optimal post-nodal lymphatic network structure that maximizes active propulsion of lymph. Am J Physiol (Heart Circ Physiol). 2009; 296:H303–H9. [PubMed: 19028799]
20. Eisenhoffer J, Elias RM, Johnston MG. Effect of outflow pressure on lymphatic pumping in vitro. American Journal of Physiology (Regulatory Integrative Comp Physiol). 1993; 265:R97–R102.
21. Eisenhoffer J, Lee S, Johnston MG. Pressure-flow relationships in isolated sheep prenodal lymphatic vessels. American Journal of Physiology - Heart and Circulatory Physiology. 1994; 267:H938–H43.

Author Manuscript

Author Manuscript

Author Manuscript

Highlights

- Contractile lymphatic vessels can be characterised by their pump function curve.
- Pump curve shape depends sensitively on the muscle length/tension relation.
- Active tension cannot be measured at all lengths as contracted/passive difference.

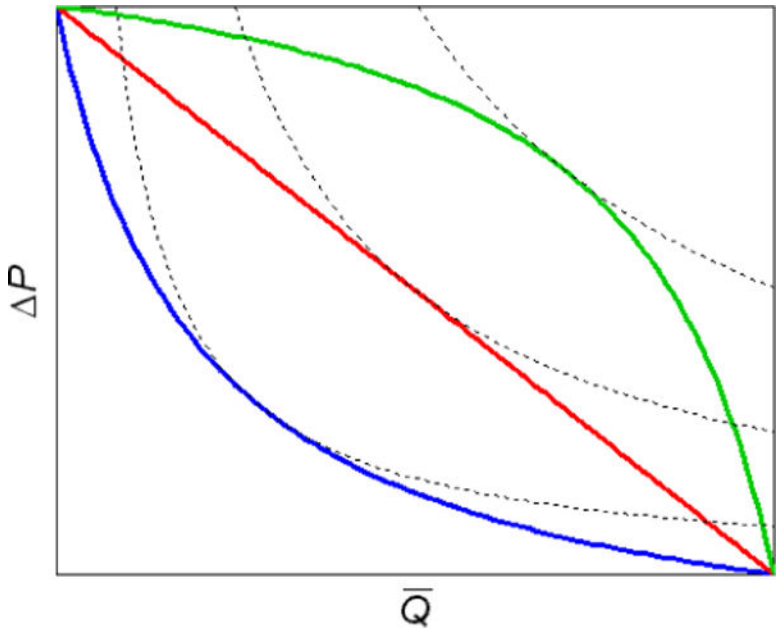

Figure 1.

Three theoretically possible shapes for a pump-function curve, each describing a different pump. Also shown are curves of constant power (the product of $\bar{Q}$ and ΔP) which are tangent to the three pump-function curves at their respective points of maximum power. The maximum power increases from blue to red to green, although all three pumps work within the same limits of maximum $\bar{Q}$ and ΔP.

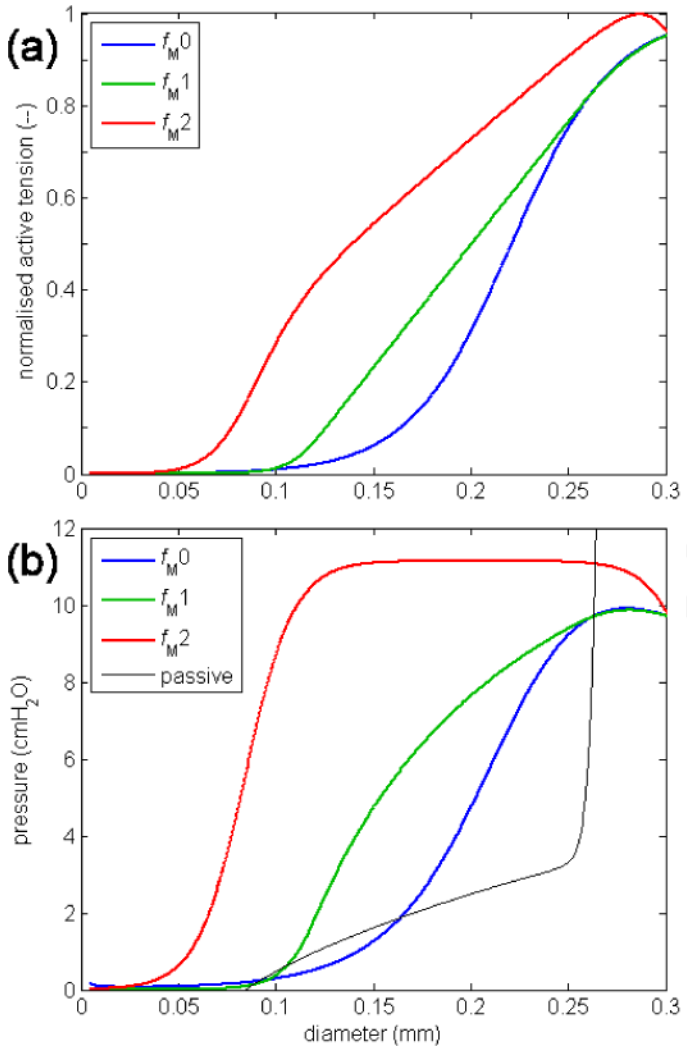

Figure 2.

The three proposed forms for the variation of active tension with lymphangion diameter. (a) Normalised active tension, $M_d(D)/M_0$. (b) Active tension converted to its equivalent in transmural pressure contribution as $2M_d(D)/D$, for peak active tension M_0 = 150 dyn/cm. It can thereby be directly compared with the passive $\Delta p_{tm}-D$ relation (thin black curve) fitted to the data of Davis et al. [6]. The f_M0 relation (shown in blue) was previously used [8] with M_0 = 250 dyn/cm. The red curve has a higher maximum because the underlying normalised active tension peaks at a lower diameter.

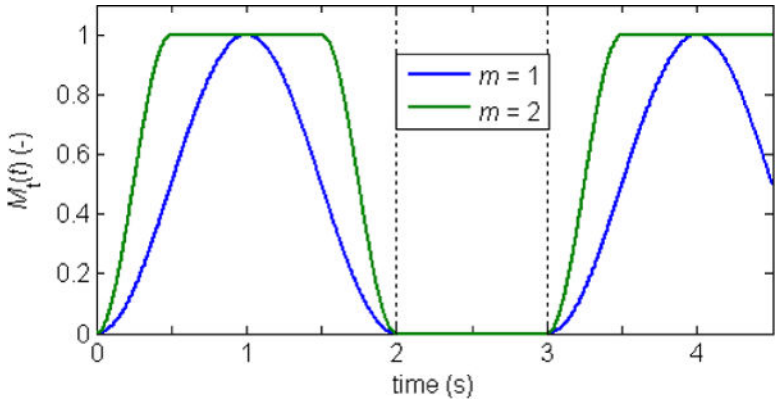

Figure 3.

Waveforms of $M_t(t)$ with a 1s refractory period and either a simple sinusoidal contraction ($m = 1$) or twice the rate of rise and fall ($m = 2$).

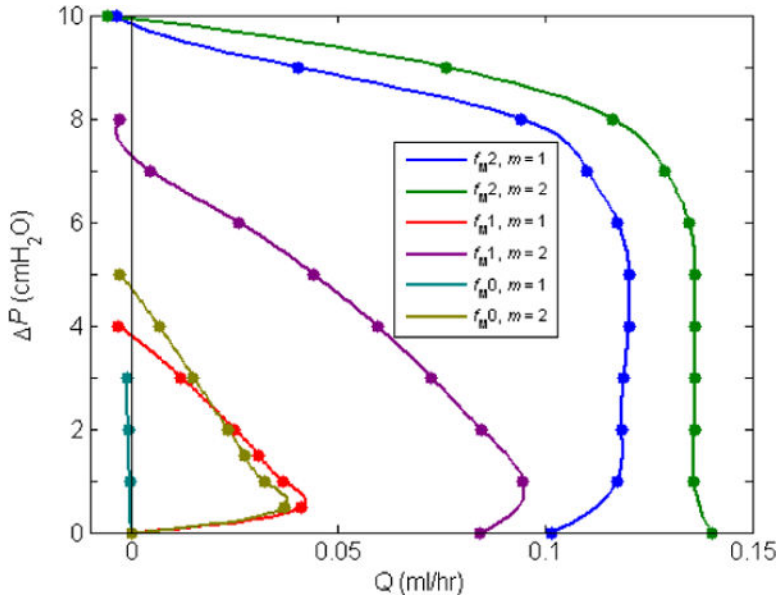

Figure 4.

Pump function curves for each of the three $M_d(D)$ relations of Fig. 3, combined with either of the two $M_t(t)$ waveforms of Fig. 3.

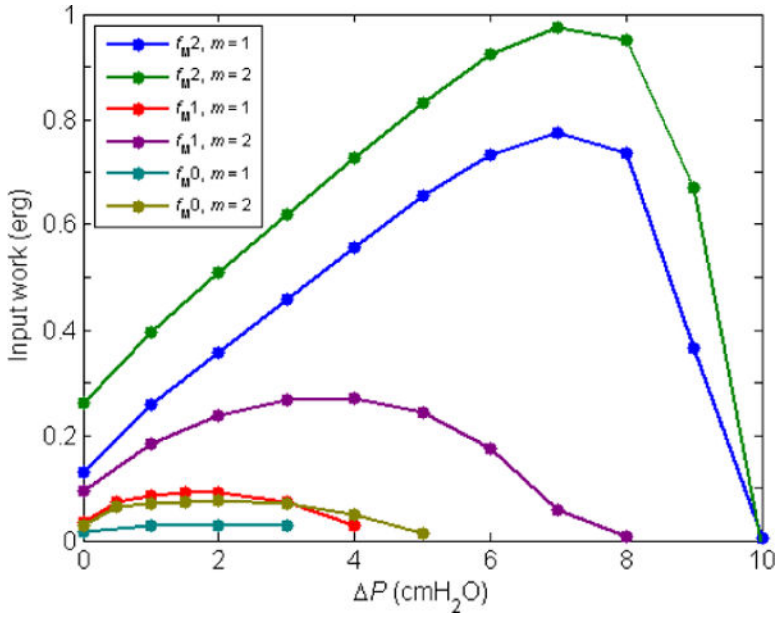

Figure 5.

Work done by active tension on the fluid contents of the lymphangion per cycle of contraction, for each of the data points shown in the pump function curves of Fig. 4.

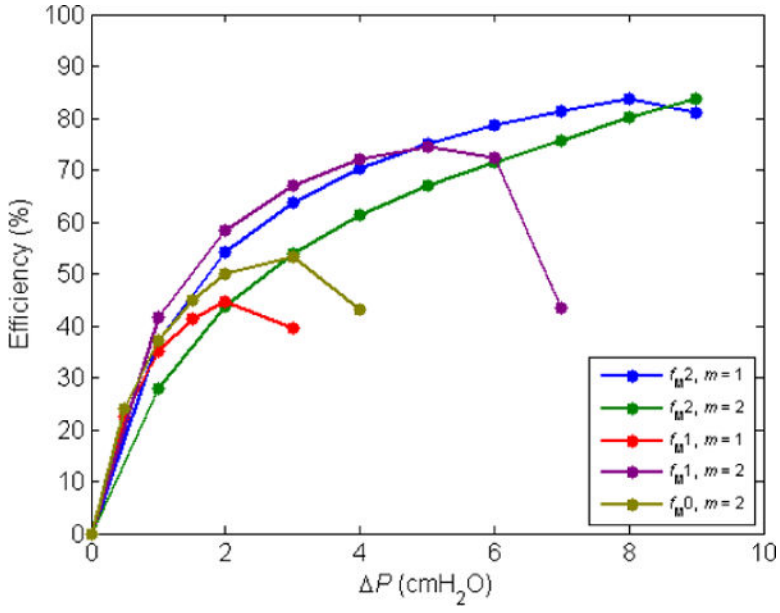

Figure 6.

The mechanical efficiency of contraction, for each of the data points shown in the pump function curves of Fig. 4 that yielded positive $\bar{Q}$.

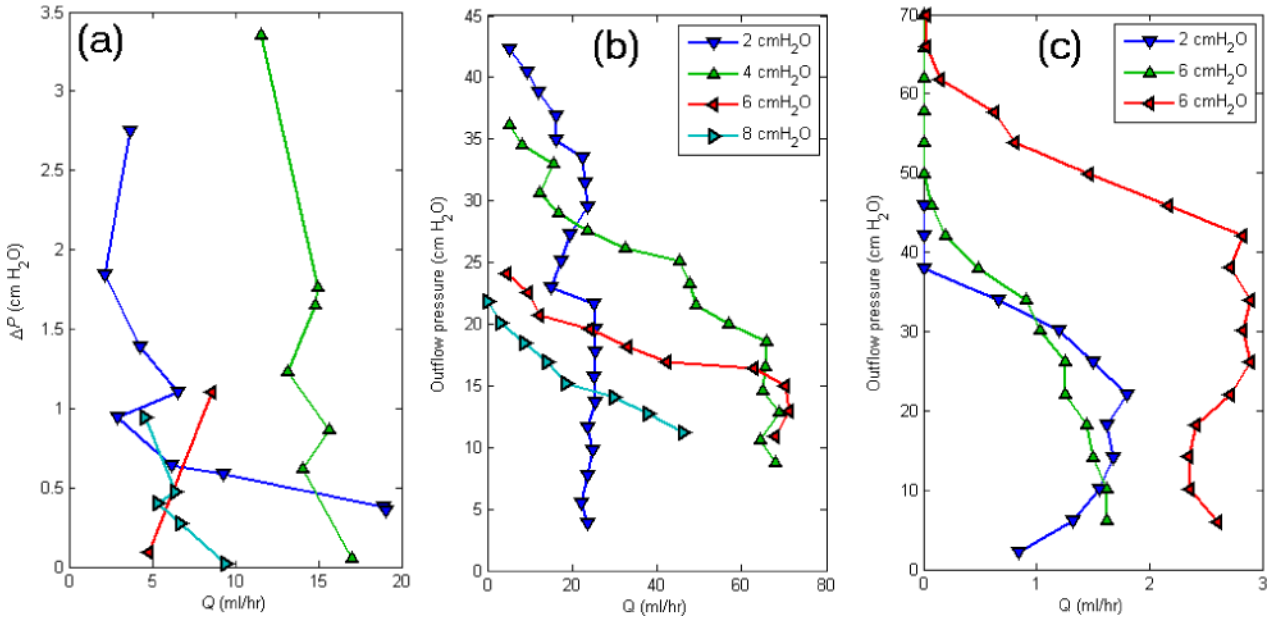

Figure 7.

(a) Pump function for bovine mesenteric lymphatics *in vitro* [19]. (b) Pump function, one bovine mesenteric vessel [20]. Transmural pressure as indicated in the legend. (c) Pump function, three ovine prenodal popliteal vessels [21]. Inflow pressure as indicated in the legend.

Table 1

Default parameter values, and the typical ranges of ΔP and $\bar{Q}$ which result. The middle column gives values in the units which are commonly used in lymphatic vascular research; for those quantities which have units, the right-hand column gives their SI equivalents.

number of valves	2	
lymphangion length, L (cm)	0.3	3×10^{-3}
normalising diameter, c_9 (cm)	0.02598	2.60×10^{-4}
diameter at $\Delta p_{tm} = 0$, D_d (cm)	0.0084534	8.45×10^{-5}
p-scale in $\Delta p_{tm}-D$ relation, P_d (dyn cm^{-2})	732	73.2
peak active tension, M_0 (dyn cm^{-1})	150	0.15
contraction waveform frequency, f (Hz)	0.5	0.5
$M_t(t)$ rise/fall-rate multiplier, m	1 or 2	
refractory period, t_r (s)	1	1
valve state-change offset from $\Delta p_V = 0$	= f(valve state, Δp_{tm})	
valve-closure slope const., s_0 (cm^2 dyn^{-1})	0.4	4
min. valve resistance, R_{Vn} (dyn cm^{-5} s)	6×10^5	6×10^{10}
Δ(valve resistance), R_{Vx} (dyn cm^{-5} s)[7]	$10^{10} - R_{Vn}$	$10^{15} - R_{Vn}$
valve-closure threshold factor, c_{fact} [8]	0.221	
lymph viscosity, μ (Poise)	0.01	10^{-3}
default $\Delta p_{ae} = p_a - p_e$ (dyn cm^{-2})	3924 (4 cmH_2O)	392.4
typical maximum $\Delta P = p_b - p_a$ (dyn cm^{-2})	9810 (10 cmH_2O)	981
typical maximum $\bar{Q}$ (cm^3 s^{-1})	2.78×10^{-5} (0.1 ml/hr)	2.78×10^{-11}

[7]Maximum valve resistance $R_{Vn} + R_{Vx}$ is thus 10^{10} dyn cm^{-5} s (10^{15} in SI units).